Cancer cells are selectively eliminated through UPR driven apoptosis during treatment with Aquilegia nivalis extracts

Nazia Hilal
University of Kashmir, Srinagar
Ozaira Qadri
University of Kashmir, Srinagar
Irshad A Nawchoo
University of Kashmir, Srinagar
Seema Akbar
Regional Research Institute of Unani Medicine, University of Kashmir Campus
Khalid Majid Fazili (fazili@kashmiruniversity.ac.in)
University of Kashmir, Srinagar

Research Article

Keywords: Aquilegia nivalis, UPR, IRE1α, XBP1, eIF2α, ATF4, Apoptosis

Posted Date: March 10th, 2021

DOI: https://doi.org/10.21203/rs.3.rs-234542/v1

Cancer cells are selectively eliminated through UPR driven apoptosis during treatment with *Aquilegia nivalis* extracts

Nazia Hilal[1#], Ozaira Qadri[1], Irshad A Nawchoo[2], Seema Akbar[3] and Khalid Majid Fazili[1*]

[1]Department of Biotechnology, University of Kashmir, Srinagar-190006, Jammu and Kashmir

[2]Department of Botany, University of Kashmir, Srinagar- 190006, Jammu and Kashmir

[3]Regional Research Institute of Unani Medicine, University of Kashmir, Srinagar-190006 , Jammu and Kashmir

Current address

Department of Biochemistry and Molecular Genetics

University of Illinois, Chicago

***Correspondence:**

Dr. Khalid Majid Fazili, PhD

Professor, Department of Biotechnology

University of Kashmir, Srinagar-190006, Jammu and Kashmir

Tel: +91-9419003881

Email: fazili@kashmiruniversity.ac.in

ABSTRACT:

Background

Aquilegia nivalis Flax Jackson, also called *Aquilegia vulgaris* sub sp. nivalis (Bak.) Brühl or columbine, locally known as “Zoe-neel”, is a wild edible plant traditionally used as an anti-inflammatory medicine by the local nomadic tribes inhabiting the Himalayas of Jammu and Kashmir. The plant has been used as herbal medicine since middle ages in treating ailments that include chronic rhinitis and various infectious diseases. The extracts from the plant possess antioxidant properties and have been reported to be hepatoprotective in rats. Our preliminary studies, however pointed to hitherto unexplored anti-apoptotic potential of the plant which lead us to carry the in-depth study using breast cancer cell lines to validate its anti-cancerous properties and explore the affected pathways.

Methods

MTT assay was used to draw the dose response curve and evaluate the effect of increasing concentrations of the extract on cell lines to determine the appropriate dosage to be used for further experimentation. DNA fragmentation analysis was followed through gel electrophoresis and DAPI staining was pursued by phase contrast microscopy to study apoptosis. Quantitative PCR was used to study the expression of UPR signaling and RIDD markers at the level of mRNA. Western blot analysis was used in studying the expression of the various markers of the signaling pathways. The cell cycle analysis was carried out using flow cytometry.

Results

MTT assay revealed that the methanolic extract of the plant (ANME) was selectively cytotoxic to various cancer cell lines as revealed by lower IC50 values relative to normal cell lines. The results of cell cycle analysis were similar as ANME caused Sub G1 arrest of the cell cycle. DNA fragmentation analysis, DAPI staining and western blot analysis

for PARP and caspases revealed that the extract selectively induced apoptosis in cancerous cell lines. UPR markers p-Ire1α and Xbp1 splicing were consistently alleviated in a dose dependent manner, the rate of phosphorylation of eIF2a and ATF4 also decreased with increasing concentration of ANME. The RT PCR results of the RIDD marker, Blos1S1 revealed a similar dose dependent association. The methanolic extract was especially chosen for it could be easily internalized by the cells and any resultant potential bioactive compounds could gain access to the cells because of their hydrophobic nature.

Conclusion

Our results suggest that ANME causes deactivation of UPR signaling pathway facilitating apoptosis selectively in cancerous cells, paving the way forward for a novel approach in cancer therapeutics.

Keywords: Aquilegia nivalis, UPR, IRE1α, XBP1, eIF2α, ATF4, Apoptosis

Abbreviations:

UPR , Unfolded protein response: ATF4, Activating transcription factor 4: ATF6, Activating transcription factor 6: GADD34, Growth arrest and DNA damage 3: XBP1, X-box binding protein 1: ANME, *Aquilegia nivalis* methanolic extract : RIDD, Regulated IRE1-dependent decay of mRNA

Introduction

The exploration of natural products offers great opportunity to researchers in medical sciences to identify and explore nature friendly therapeutic agents relevant to different diseases. Aquilegia nivalis is a traditional indigenous herb found in higher altitudes of Himalayas[1]. The plant has been traditionally used in treatment of Asthma and as an anti-inflammatory agent. It is also used as a remedy for many ailments including chronic rhinitis and various infections[2]. The extracts of the plant [plant extract] have shown hepatoprotective effects in mice.[3] Several studies have shown the anti-oxidant role of the

plant.[4,5]. Despite of its well-known anti-inflammatory and anti-oxidative properties, and the fact that the plant has been used for a long time as a traditional therapeutic agent in treating several disorders like bronchitis and bowel disorders, the plant has not been explored to its full potential. No study has been carried out to find its molecular targets and the mode of action. The plant is being extensively used by the nomadic tribes inhabiting the Himalayan ranges in Jammu and Kashmir. Some studies have suggested the antiproliferative and pro-apoptotic activities of the plant[6]. Our preliminary data indicated that the plant extracts were selectively toxic to cancerous cells, so the current study was carried out to validate the antiproliferative potential of the plant and explore its molecular targets in the cell. The study revealed that the methanolic extract of the plant affected UPR signaling and RIDD pathways.

The unfolded protein response is a defensive mechanism that gets activated under stressful conditions to restore homeostasis, during prolonged stress however, when restoration becomes difficult, it promotes apoptosis[7]. The synthesis and trafficking of nearly one-third of the total protein in eukaryotic cells is synchronized by Endoplasmic Reticulum[8,9,10]. The ER is responsible for tuning up protein homeostasis[11] and ensures the release and bartering of properly folded proteins after post-transcriptional and post-translational modifications through various mechanisms existing within the organelle. Despite this, a colossal amount of proteins transiting via ER are not properly folded and may be degraded by ER-associated degradation (ERAD) system[11]. The perturbations in influx to efflux ratios of proteins within the ER compartment coupled with accumulation of misfolded proteins causes ER stress that is combated through a defensive mechanism known as Unfolded Protein Response[12,13]. UPR determines the cellular fate either towards survival or death depending upon the severity of stress and primarily operates via three axis namely; Ire1-α/Xbp-1, PERK/eIF2α and ATF6 [7,14,15]

Tumor cells experience increase metabolic activities and high proliferation rates, which in turn demands boisterous ER and secretory mechanisms. This boosted demand for secretory functions is likely to trigger a mid-course correction of ER homeostasis and consequently ends up in basal or constitutive UPR induction. Ire1α mutations have been implicated in many human cancers on the basis of genome wide screening with roles in tumor growth, metastasis and chemo-resistance[16,17,18.] A compromising tumor growth and survival is observed when Xbp1 expression is thwarted, inhibiting Ire1/Xbp1 axis impinge the coherence of the secretory tissues [19-23]. PERK pathway in tumor cells either facilitates their survival or suppresses their progression. PERK branch confers oncogenic transformation by promoting myc induced autophagic pathways[24,25]. CHOP (an apoptosis mediator) suppresses the tumor progression thus chop deletion has tumor progression phenotype in lung cancer.[26,27]

Many pathological complications are associated with the disturbance in the protein folding machinery, aggregation and concurrent ER stress[7,28]. Various therapeutic drugs induce ER stress and destine the cells to apoptosis[29]. It is possible that an optimum level of ER stress and UPR signaling is induced under tumor microenvironment is necessary for cancer survival and progression, but exacerbating the stress levels beyond the handling capacity can drive cancer cells toward death. UPR signaling can be targeted in cancer treatment in both ways, that is, either by inducing a high level of stress in the pre-existing stress microenvironment of tumor or by preventing activation of UPR that is beneficial for cancer progression and drug resistance, making them sensitive to other chemotherapeutic drugs.

In the above context, our study becomes important as it reflects the potential effects of the plant extract to selectively induce apoptosis in cancerous cells coupled with deactivation of UPR and RIDD signaling pathways.

MATERIALS AND METHODS:

Chemicals

Tunicamycin was purchased from EMD Millipore (Darmstadt, Germany).Dulbecco's modified Eagles medium (DMEM) and Fetal bovine Serum (FBS) were purchased from GIBCO (St. Louis, Mo, USA). Bicinchoninic acid (BCA) protein assay kit was purchased from pierce (Rockford, USA). and 3-(4,5-dimethylthiazole-2-yl)-2,5, diphenyltetrazolium bromide (MTT) were purchased from Sigma-Aldrich (St. Louis, Mo, USA).

Preparation of methanolic fraction of *Aquilegia nivalis*

Aquilegia nivalis was collected between July and August 2016, from several regions of Kashmiri Himalayas. The plant was identified and deposited in the KASH Herbarium under voucher specimen No.2716-(KASH). Whole Plant parts were washed with distilled water to remove residues and shade dried. The dead parts were removed, and healthy ones were grounded to powder, preserved for extraction. ANME (Methanolic fraction of *Aquilegia nivalis*) was prepared from dried and coarse powder using methanol as a solvent. Hot extraction was carried out in a Soxhlet apparatus taking Plant powder and solvent in ratio of 1:6. The extract was filtered and evaporated to dryness and the residues were weighed. The extract solutions obtained were combined and evaporated to dryness by a rotary evaporator under vacuum at 65 °C. The yield was calculated by dividing the mass of recovered dry extract (mr) by the initial mass of powder (mi).

$$\text{Yield}(\%) = mr/mi \times 100\%$$

This residue was then dissolved in 50% DMSO to make the concentration of 100 mg/mL working stock and stored at 4°C. The working concentration of DMSO used was 2% for experiments.

Cell lines

Breast cancer cell lines, MDAMB-231 and MCF7 and neuronal cell line U87MG glioblastoma, and the normal human embryonic kidney cells, Hek293T were purchased from National Centre for Cell Science (NCCS, Pune).

Antibodies and Western blot analysis

SDS-Polyacrylamide gel electrophoresis and Western blotting were performed by usual procedures . All the four cells were seeded at 1×10^6 cells/well in a 100 mm culture dish and incubated for 24 h. The incubated cells were treated with varying concentrations of ANME with or without 6μM of tunicamycin for 24 h. The cells were harvested in phosphate buffered saline (PBS) containing 0.1% protease inhibitor cocktail. The primary and secondary antibodies used were as follows. Rabbit polyclonal antibodies against Phosphorylated version of Inositol requiring enzyme (Ire1α), X-box binding protein spliced (sXbp1), Activating transcription factor 4 (ATF4), Phosphorylated version of alpha subunit of eukaryotic initiation factor (p-eIF2α) and GAPDH were obtained from Cell Signaling Technology (Danvers, MA). Alkaline Phosphatase linked secondary anti-Rabbit antibody was purchased from Sigma-Aldrich (St. Louis, Mo, USA). BCIP (5-Bromo-4-chloro-3-indolylphosphate) and NBT (Nitro blue tetrazolium) were purchased from Sigma-Aldrich (St. Louis, Mo, USA).

Real-time quantitative PCR for analysis

The cells were seeded at 1×10^6 cells/well in a 100 mm culture dish and incubated for 24 h. The incubated cells were treated with varying concentrations of ANME with or without 6μM of tunicamycin for 24 h. RNA was extracted from the harvested cells using an RNeasy kit (Qiagen, Hilden, Germany). RNA was reverse-transcribed to synthesize cDNA using a Revert Aid First strand cDNA synthesis kit (Thermo scientific) as per manufacturer's protocol., and used in duplicate for quantitative real-time PCR analysis using the SYBR Green reagent system Applied Biosystems 7500 Fast Real-Time PCR

System (Applied Biosystems, Foster City, CA). Relative quantities of amplified cDNAs were then determined using SDS software (Applied Biosystems) and normalized to β-actin mRNA.

The following primers were used:

ATF4

5′-TTC CTG AGC AGC GAG GTG TTG -3′(sense)

5′-TCCAATCTGTCCCGGAGAAGG-3 (antisense)

CHOP

5/-CTTGGCTGACTGAGGAGGAG-3/(sense)

5/-TCACCATTCGGTCAATCAGA-3/(antisense)

Spliced XBP1

5 /-CTGAGTCCGAATCAGGTGCAG-3/(sense)

5/-ATCCATGGGGAGATGTTCTGG-3/(antisense)

β-actin,

5/-TCATCACCATTGGCAATGAG-3/ (sense)

5/-CACTGTGTTGGCGTACAGGT-3/ (antisense)

Quantification of western blot

The intensity (area x optical density) of the individual bands on Western blots was measured by using ImageJ and normalized either to GAPDH or, in the case of a phosphoprotein, to its total protein as mentioned.

Cell viability assays

Cell viability measurements for ANME were done using MTT assay. Cell were seeded in 96-well plate at 10^4 cells per well. Different concentrations of extract (1-2000µg/mL) were added to each well incubated for 24 h. Next day 10 µL of 5 mg/mL MTT were added to each well and incubated for 4 h. The formazan crystals were dissolved by adding 100 µL of DMSO to each well. Absorbance was measured at 560 nm with

Universal Microplate Reader (Bio-Tek Instruments, USA). The reference wavelength was set at 650 nm. The cell viability of untreated cells was considered 100%.

Cell cycle analysis by flow cytometry

The cells were seeded at 1×10^6 cells/well in a 100-mm culture dish and incubated for 24 h. The incubated cells were treated with ANME (50 µg/mL for MDAMB231 100 µg/mL for MCF7 and 25 µg/mL for U87MG), with or without 6µM of Tm for 24 h.. Media was collected in 15ml tubes and cells were washed with PBS containing 0.1% EDTA. Washing solution was also collected. PBS-EDTA was added to the plates followed by incubation at 37 °C for 5-10 minutes. Cells were collected, pipetted up and down and collected in same tubes. Tubes were centrifuged at 1000 g for 5 minutes followed by washing in PBS-Serum (1% serum) and centrifuged again at 1000g. Afterwards, cells were resuspended in 0.5 ml PBS. For fixing, 5 ml ethanol was added drop wise while vertexing the cells. Cells were then stored in deep freezer for FACS analysis. For FACS analysis, fixed samples were centrifuged at 1000g for 5 minutes and washed with PBS-serum followed by resuspension in Propidium Iodide-RNAse solution (50 µg/ml propidium iodide, 10mM Tris pH 7.5, 5 mM MgCl2 and 20 µg/ml RNase A). Finally, samples were acquired and analyzed by using BD FACS machine and BD FACS Suite software. The experiments were done in triplicates. For analysis outliers were discarded.

Statistical analysis

The GraphPad Prism®6 software (GraphPad software Inc.) was used for statistical analysis. All experiments were repeated independently three times. IC50 values were also calculated using non-linear regression analysis with GraphPad Prism®6 software.

Results

ANME display cytotoxicity against cancer cell lines in vitro

MTT viability assay on HEK293T human embryonic kidney cells, MDAMD-231 breast cancer,MCF7 breast cancer and U87 glioblastoma cells were done separately with a

range of concentrations of ANME between 1 to 2000 µg/ml. ANME alleviated cell viability in a dose dependent manner. All the experiments were performed in triplicate. IC50 values were calculated by non-linear regression analysis using Graph Pad Prism software as a mean of three reactions that inhibited 50% of the positive control. The IC50 values of ANME in HEK293T human embryonic kidney cells, MDAMD-231 breast cancer, MCF7 breast cancer and U87 glioblastoma were 532.1µg/mL, 100.2µg/mL, 205.6µg/mL and 42.23µg/mL, respectively (Fig.1A-D). Higher concentrations of the extract presented with vivid morphological changes under phase contrast microscope. The most marked changes were cell shrinkage and extensive cell detachment from cell culture substratum.

ANME displayed different cell cycle responses

The propidium iodide based cell cycle analysis by flow cytometry revealed that the cell lines responded differently to the treatment with some cells undergoing significant cell death, as indicated by an increase in SubG1 peak, whereas others not showing any appreciable change in the cell cycle profile. HEK 293T (human embryonic kidney) cell line which is a normal cell line didn't show an appreciable increase in SubG1 peak (Fig. 2 A). U87MG (human glioblastoma) cell line showed moderate response to ANME treatment (Fig. 2 B). MDAMB231 and MCF7 (Breast cancer) cell lines, however, showed a remarkable increase in SubG1 (Fig. 2 C-D). This indicated that the breast cancer cell lines were highly sensitive to ANME treatment. These results show that different cell types respond differently to ANME, whereas different cancer cell lines are sensitive to a varying degree, the response ranging from low to high cell death, the normal cell lines did not show any significant effect.

ANME inhibits tumor cell growth in vitro by induction of apoptosis

The antiproliferative potential of ANME was evaluated in HEK293T human embryonic kidney cells, MDAMD-231 breast cancer, MCF7 breast cancer and U87 glioblastoma. As

shown in Fig 1A IC50 values of HEK293T human embryonic kidney cells, MDAMD-231 breast cancer, MCF7 breast cancer and U87 glioblastoma for ANME treatment were 532.1µg/mL, 100.2µg/mL, 205.6µg/mL and 42.23µg/mL, respectively revealing a relatively higher sensitivity of cancer cell lines. Also there was a general SubG1 arrest in the cells. The Ladder assay revealed a time-dependent increase in DNA fragmentation on treatment with ANME as observed on DNA-gel electrophoresis. DNA extracted from cells treated with ANME showed an increased generation of apoptotic DNA fragments as compared with solvent-treated control cells, it also displays a higher sensitivity of the cancer cell lines relative to normal cell lines.(Fig. 3A)

DAPI assay revealed apoptosis-specific features of ANME-treated cells from 0 Hours to 48 Hours. U87 MG, MDAMB231 and MCF7 on treatment with ANME showed various nuclear changes such as chromatin condensation, nuclei condensation, and nuclear degradation, however Hek293T cells did not show any signs of significant apoptotic activity. (Fig. 3B)

UPR mediated onset of Apoptosis

Since the cancerous cells are in a state of constant stress because of their high metabolic profile, controlled UPR is known to be active in these cells. So next we decided to look at the UPR signaling pathway. Figures 4-7 show the results of Western blots of various UPR signaling markers using specific antibodies. In order for us to check the pathway involved through which ANME caused the apoptosis, we checked for the global impact on proteostasis markers. The perturbation of cellular proteostasis networks by inhibition of the proteasome results in induction of an unfolded protein response[30,31]. Our results suggested that ANME averted UPR response in both Cancer and 293T cells, as judged by inhibition of p-Ire1α. Figure 4 shows the effect of tunicamycin and increasing concentrations of ANME on the expression of phosphorylated Ire1α. The phosphorylation of Ire1α causes activation of UPR and serves as one of the first markers

of UPR activation. As is shown in figure, ANME exposure is associated with decreasing concentration of P-Ire1α in all the four cell types (Fig. 4 A-D) reflecting deactivation of the kinase associated IRE1 signaling of UPR. Xbp1s is another downstream marker of the same pathway. Figure 5 shows the effect of tunicamycin and increasing concentrations of ANME on Xbp1 splicing. ANME inhibits the splicing reaction in all the cell types as indicated by reduced expression of XBp1-s.(Fig.5 A-D), the total phosphorylation level of Ire1α protein decreased, with kinetics matching the inhibition of Xbp1s, consistent with a previous report[32].

Next, we evaluated the effect on the PERK arm of UPR. Figure 6 shows the effect of tunicamycin and increasing concentrations of ANME on the expression levels of p-eIF2α and ATF4, the downstream effector molecules of the PERK arm of UPR The expression levels of both the effector molecules decreased in a concentration dependent manner on treatment with ANME (Figure 6 A-D)

Further we tested the effect of ANME treatment on mRNA expression levels of Xbp1 and ATF4 in different cell lines. ANME significantly repressed the expression of Xbp1, a downstream target of Ire1 arm, and ATF4, a downstream target of PERK arm of UPR in a concentration dependent manner (Figure 7 A-C)

Next we checked effect of the treatment on RIDD activity. Figure 8 shows the qRT PCR based mRNA expression of BLOC1S1 (BLOS1) which is used as a marker for RIDD activity. Treatment with increasing concentrations of the extract shows a 2-3-fold increase in the expression levels in all the cell lines tested (Figure 8 A-C) indicating that the RIDD arm of UPR is also decreased. To check whether ANME directly inhibits Ire1α activity, we tested ANME inhibition on RIDD marker BLOC1S1 (BLOS1) which are considered as standard markers for testing RIDD activity.[33,34] We found that ANME inhibit Ire1α activity in vitro for RIDD (Fig 8 A-C), indicating the role of ANME on in apoptosis is through the RNAse activity of Ire1α in a dose-dependent manner.

ANME-induced apoptosis of tumor cells is associated with dual inhibition of Ire1/xbp1 and PERK/ATF4 and activation of Caspases

Following DNA ladder assay and cell cycle analysis, we probed the effect of ANME on caspase and PARP. Western blots with PARP and caspase antibodies were used to probe the effect of the treatment with different cell lines. The results are shown in Figure 9. HEK293T cell lines did not show any apoptotic signals as revealed by the absence of caspase3 and PARP (Fig.9A), however, other cell lines U87MG, MDAMB231 and MCF7 clearly show the onset of apoptosis in a concentration dependent manner (Figure 9 B,C). This was consistent with the results obtained in DNA fragmentation assay and cell cycle analysis. This can be attributed to the fact that in HEK293T cells the Unfolded Protein Response is rescued due to ANME treatment resulting in restoration of the in milieu proteostasis. However, the apoptotic death in other cell lines that are cancerous in nature is ascribed to uncompromised ER stress associated with activation of the RIDD pathway. These results suggested the pro-apoptotic potential of ANME is attributed to the dual inhibition of Ire1/xbp1 and PERK/ATF4 axis that renders the cancer cells vulnerable to apoptotic death via activation of caspases.

Discussion

Aquilegia nivalis traditionally used in treatment of asthma and ailments like chronic rhinitis and infections with documented hepatoprotective properties offers great promise in disease therapeutics. The plant though has not been explored to its full potential. The extracts of the *Aquilegia* species have been shown to display hepatoprotective effects in mice.[3, 35,36] Several studies have shown the anti-oxidant activities of the plant. The plant has been used as a herbal medicine since ages with proven efficacy in diseases like chronic rhinitis, and as anti-inflammatory in infections.[4,5,36] However detailed studies validating the therapeutic potential of the plant and about the mode of its action are lacking. This study was conducted to validate its antiproliferative effects and evaluate its

target signaling pathways as anti-inflammatory activities in certain plants are reported to be coupled with anti-proliferative pro-apoptotic activities[6]. Our preliminary investigations on the extracts of the plant showed that the methanolic extract of the plant selectively acted on cancer cells. Based on this we carried in-depth study on several cancer cell lines with promising results. This study established that the extract from the plant selectively induced the apoptotic pathways leading to cell death in cancerous cells. The methanolic extract from the plant was particularly chosen for it displayed higher activity and for the fact that it could easily be internalized by the cells. Any potential bioactive compounds could also be easily accessible to the cells because of their hydrophobic nature. In the ladder assay, DNA fragmentation followed by gel electrophoresis revealed generation of apoptotic fragments selectively in cancerous cells and also an alleviation of apoptosis is observed on treatment with the methanolic extract of Aquilegia nivalis in a concentration dependent manner. Cell cycle analysis with flow cytometry displayed a differential response of the cells, whereas subG1 arrest was observed in all the cancerous cells but with variations in the subG1 peak, the normal cells behaved differently with no subG1 peak observed. DNA fragmentation and cell cycle arrest have been considered a hall mark of apoptosis [33]. Other pro-apoptotic markers that were tested include Caspase-3 and PARP which showed comparable results with different cancerous cell lines experiencing apoptosis to variable degrees, though no significant amount of apoptosis is seen in normal cell lines. Several recent studies have demonstrated the proapoptotic and anti-apoptotic potential of plant derived extracts[34,37,38]. The methanolic extracts of *Andrographis nallamalayana Ellis* have been shown to induce apoptosis in various melanoma cell lines [6]. Similarly extracts derived from *Menyanthes trifoliata* L. are reported to induce apoptosis in human cancer cells affecting Caspase 3, PARP and other pro apoptotic markers in a similar fashion[39]. Next we tried to understand the affected pathways. Cancer cells are under constant stress due to their high metabolic load, and the

link between the cellular stress response and apoptosis is relatively well established. Many studies have linked modulation of unfolded protein response to apoptosis[40,41]. Under hypoxia, cells have been found to show upregulation of hypoxia induced proteins and UPR signaling cascade that differ in normal and cancerous cell lines, however, the exact mechanism deciding about the cell fate is not clearly understood[42]. Next we checked the expression of downstream molecules of the Ire1 and PERK arms of the UPR signaling pathway as well as BLOS1, a marker for RIDD activity.

It was found that treatment of cells with the methanolic extract of the plant downregulated the phosphorylation of Ire1 alpha and Xbp1 splicing in a concentration dependent manner. It also resulted in reduced protein expression levels of phosphorylation levels of p-eIF2α and protein levels of ATF4 in all four cell lines viz HEK-T293, U87-MG , MCF7 and MDAMB 231. The complexity of Ire1 biology was demonstrated through a recent study suggesting that modulation of Ire1 RNase activity was possible through an allosteric mechanism using ATP-competitive kinase inhibitors APY29 and sunitinib[43]. Furthermore, a peptide derived from the Ire1 kinase domain was shown to stimulate Ire1 oligomerization while inhibiting the JNK activation and RIDD activity of Ire1[44]. Ire1 modulators specific for either Xbp1 splicing or RIDD activity may be clinically useful depending on the therapeutic intent. Protein kinase R (PKR)-like endoplasmic reticulum kinase (PERK) mediates the translational control arm of the UPR by enhancing phosphorylation of alpha subunit of eukaryotic Initiation Factor 2 (eIF2α) that kickbacks to a variety of endoplasmic reticulum stresses associated with numerous diseased states. Evidences relating PERK with tumorigenesis and cancer cell survival commoved our search for small molecule inhibitors.

The expression of Xbp1s and ATF4 was also found to be inhibited in a similar manner at mRNA level. The mRNA expression of BLOC1S1, a marker for RIDD activity was found to be increased on treatment with the extracts, owing to the fact that the extract was

downregulating RIDD activities as well. This in in line with the studies carried by These results were consistent with the protein markers of UPR signaling and RIDD activity and reflected a dual modification of the signaling by ANME treatment[45].

The unfolded protein response (UPR) serves as an adaptive mechanism to restore homeostasis. When the stress prolongs and resolution becomes difficult, the UPR commits the cell to apoptotic death. Here we show that in cancerous cells MDAMB-231 , Breast cancer cell lines, MCF7, neuronal cell line and U87MG glioblastoma, apoptotic pathways are activated via modulation of Unfolded protein response that includes inhibition of the Ire and PERK signaling as well as activation of RIDD signaling. These results point towards the cross-regulation between the apoptotic cascade and the adaptive UPR signaling in cancerous cells. Similar observations have recently been recorded with studies on Ire1 mutants [46].

An important finding of the study is that in Hek293T cells the cell death via apoptosis was not evident. This may be attributed to the fact that in these cells the UPR has being rescued due to ANME and the *in mileu* proteostasis was restored as depicted from restoration of UPR markers to the basal level, and that no Caspase 3 or PARP cleavage is seen in these cells. The apoptotic death in other cell lines cancerous in nature can be ascribed to the chronic stress conditions developing as a result of inhibition of the arms after drug treatment that in turn increases ER stress intensity to its threshold level initiating apoptosis through repression of antiapoptotic pre-miRNAs [47,48] or alternatively through upregulation of Casp2[49]. In Hek293T cells the UPR has been rescued due to ANME and the *in mileu* proteostasis was restored as depicted from restoration of UPR markers to the basal level and also no Caspase 3 or PARP cleavage was seen in these cells. A close association of Ire1α activity and cell fate determination has been proposed that provide evidences of Ire1α being molecular switch that facilitates apoptosis during prolonged ER stress**.** The caspase activation due to inhibition of PERK arm is in line with

earlier studies wherein deletion of PERK in MEF cells subjected to prolonged hypoxia has been reported to produce partial restoration of protein synthesis and enhanced activation of caspases, leading to elevated levels of cell death[50]. Taken together our results suggest that apoptosis is selectively induced in cancer cells MDAMB-231, MCF7 and neuronal cell line U87MG glioblastoma during treatment with *Aquilegia nivalis* extract (ANME) coupled with modulation of the Unfolded Protein Response signaling pathways with inhibition of Ire1 and PERK signaling cascades. Interestingly however the treatment also resulted in deactivation of the regulated IRE1-dependent decay of mRNA (RIDD). Further studies are required to understand the mechanistic basis of these effects and explore the therapeutic potential of the constituent bioactive molecules.

Conclusion

The methanolic extracts of *Aquilegia nivalis* selectively target cross-regulation between apoptosis and adaptive UPR signaling in cancerous cells may contain potential therapeutic molecules selectively targeting cancerous cells.

Declarations

Ethics approval and consent to participate

Not applicable

Consent for publication

All authors agree to submission of the manuscript for publication to BMC complementary medicine and therapies and give their consent for its publication, if accepted.

Availability of data and materials

The datasets used and/or analyzed during the current study are available from the corresponding author on reasonable request.

442 **Competing interests**

443 The authors declare that they have no competing interests as defined by BMC , or other
444 interests that might be perceived to influence the results and / or discussion reported in
445 this paper.

446 **Funding**

447 The study was funded by research grants from the Ministry of Ayuerveda, Yoga nad
448 Naturopathy, Unani, Siddha and Homoaepathy (AYUSH) to KMF, Grant No.
449 Z.28015/09/2016-HPC (EMR)-AYUSH-C. NH and OQ have been the recipients of
450 Senior Research Fellowship and Junior Research Fellowship respectively from the
451 Ministry of AYUSH funded project.

452 **Author contributions**

453 Nazia Hilal, Seema Akbar and Khalid Majid Fazili were involved in the concept and
454 design of the study. The acquisition and analysis of the data was done by Nazia Hilal and
455 Ozaira Qadri. Nazia Hilal wrote the main manuscript and prepared figures, KMF revised
456 the manuscript. Irshad A Nawchoo and Seema Akbar identified and the plant and were
457 involved in extraction. All the authors reviewed and approved the manuscript . The final
458 approval of the manuscript was by Khalid Majid Fazili and Nazia Hilal

459 **Acknowledgements**

460 We acknowledge the financial support provided by grants from the Ministry of AYUSH,
461 New Delhi (No.Z.28015/09/2016- HPC (EMR)-AYUSH-C) to Khalid M Fazili. Nazia
462 Hilal and Ozaira Qadri received fellowships from the Ministry of AYUSH during this
463 project. We would also like to acknowledge Department of Biotechnology (DBT), New
464 Delhi to provide grant support (No. BT/PR7240/MED/30/915/2012) to Khalid Majid
465 Fazili. We would also like to acknowledge the FIST support (No. SR/FST/LSI-384/2008)
466 from Department of Science and Technology and the facilities extended by University of
467 Kashmir, Srinagar-190006, India

Authors' information

NH has been a Ph D student and recipient of Senior Research Fellowship from Ministry of AYUSH funded project TO KMF. She is currently a Post Doctoral Fellow at University of Illinois, Chicago. NH is recipient of MSCA and DFG Fellowship. Ozaira Qadri is a PhD student and has been the recipient of Junior Research Fellowship from Ministry of AYUSH funded project sanctioned to KMF. OQ is recipient of the Senior Research Fellowship from Indian Council of Medical Research. Irshad A Nawchoo is Professor of Botany and Dean, School of Biological Sciences at University of Kashmir. Seema Akbar is a Scientist and Director In-charge of Regional Research Institute of Unani Medicine, University of Kashmir campus, Srinagar. Khalid Majid Fazili is Professor and Head of Biotechnology Department and Dean School of Unani and Ayuervedic Medicine at University of Kashmir.

FIGURES:

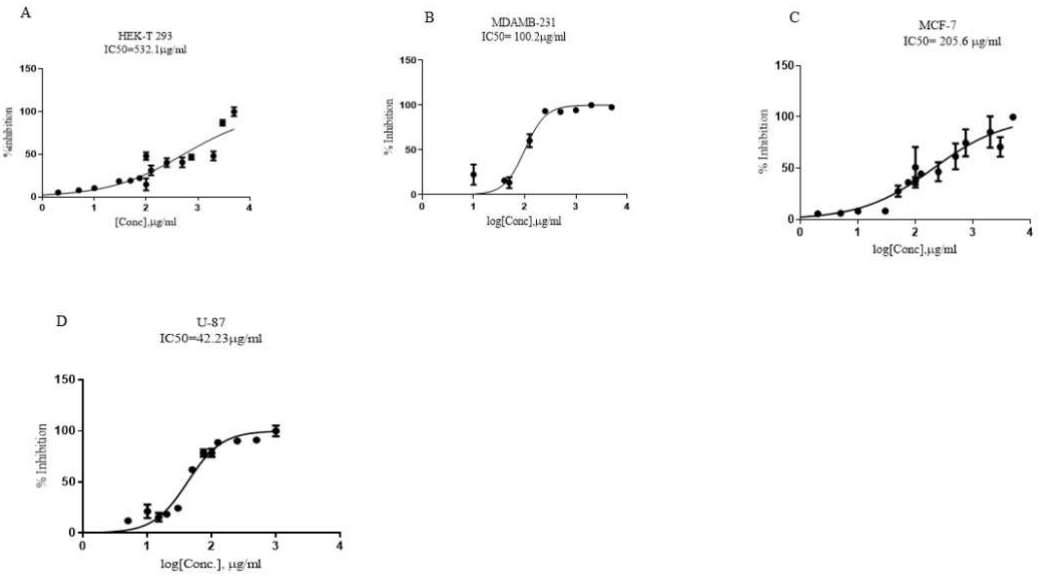

Figure.1: Effect of ANME on (A)HekT293 (B) MDAMB-231(C) MCF7 and (D) U87MG 2 cells in various concentrations (1-2000µg/mL) after 24 hours; determined using MTT cell viability assay: Dose–response curves of ANME was determined using MTT cell viability assay. IC_{50} values were calculated as mean values from three independent experiments by nonlinear regression using Graph pad Prism®6 software. Percentage inhibition of untreated cells was assumed to be zero.

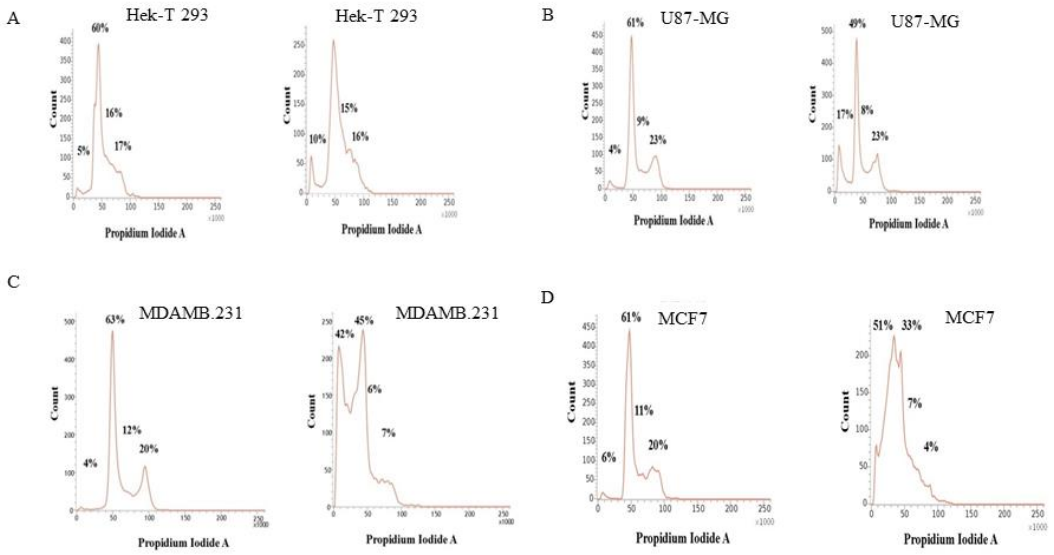

Figure.2: Cell cycle analysis: (A-D) Hek293T, U87, MDAMB-231 and MCF 7 cell lines were treated with different concentrations of ANME for 24 hrs and cells were fixed and stained with propidium iodide and analyzed by flow cytometry. The mean values ± SD were calculated from three different experiments. $p<0.05$ with respect to control.

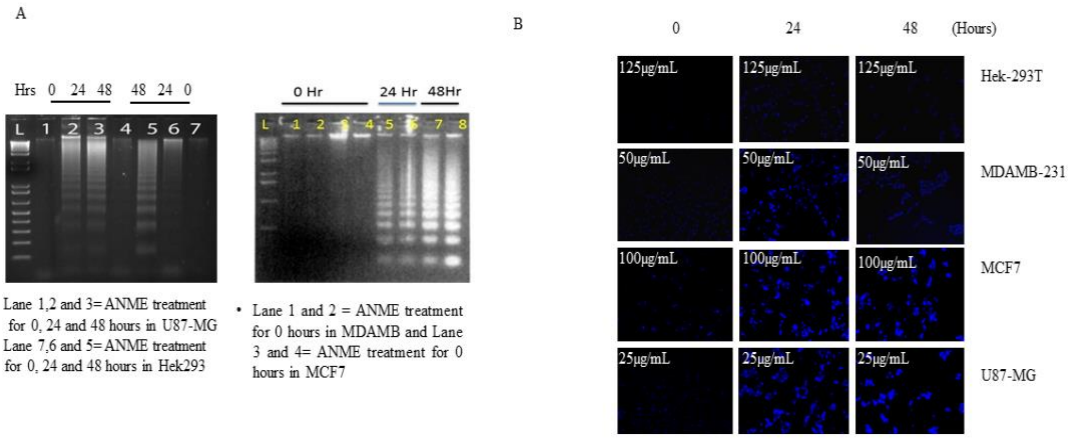

Figure.3: (A) Time dependent DNA fragmentation: DNA Laddering in (a) U87- MG and HEK-T293 cells (b) MDAMB231 and MCF7 cells resp. ANME extract induces DNA fragmentation in all the cell line panels stimulated with or without 6µM

Tunicamycin(4hr) for induction of Unfolded Protein cells. The cells were treated with different concentrations (µg/ml) of extract for every cell type for 0, 24 and 48 h. Cells from each sample were harvested for DNA gel electrophoresis as described;

(B) Formation of apoptotic bodies in time dependent manner, DAPI staining: Morphological and nuclear changes induced by ANME. HEK- T293, MDAMB, MCF7 and U87-MG cells after treatment with different concentration for each cell type induced various nuclear changes such as chromatin condensation, nuclei condensation, and nuclear degradation, as demonstrated by DAPI staining at 400× in time dependent manner. However Hek293 showed only inhibition in cell growth with no signs of apoptosis; ANME=*Aquilegia nivalis* methanolic extract.

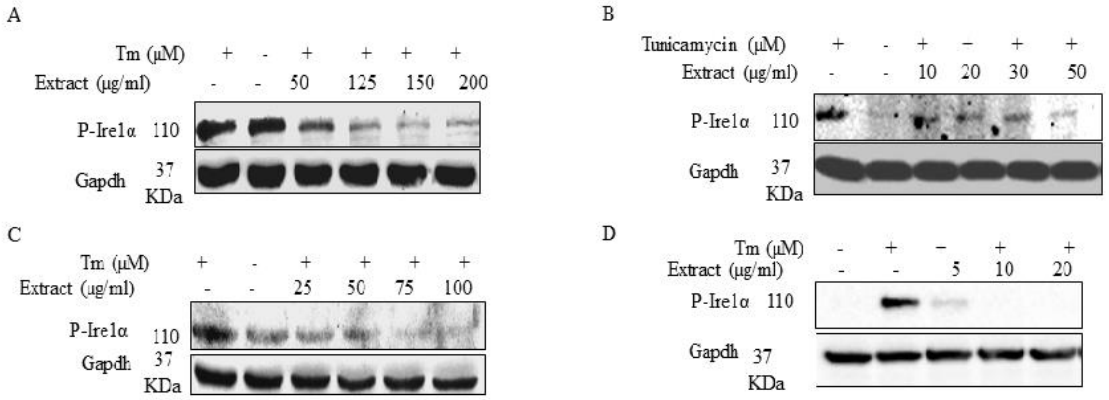

Figure.4: Immunoblot analysis for p-Ire1α in (A) Hek293T (B) MDAMB 231(C) MCF 7 (D) U87 MG: Protein extracts of Hek T 293, MDAMB 231, MCF 7 and U87MG stimulated with or without 6µM Tunicamycin (4hr) for induction of Unfolded Protein Response followed by treatment with different concentrations in µg/ml of ANME was isolated and run out for Western blotting. Blots were probed with p-Ire1 α. GAPDH was used as loading control. Experiments were repeated three times and a representative blot is shown.

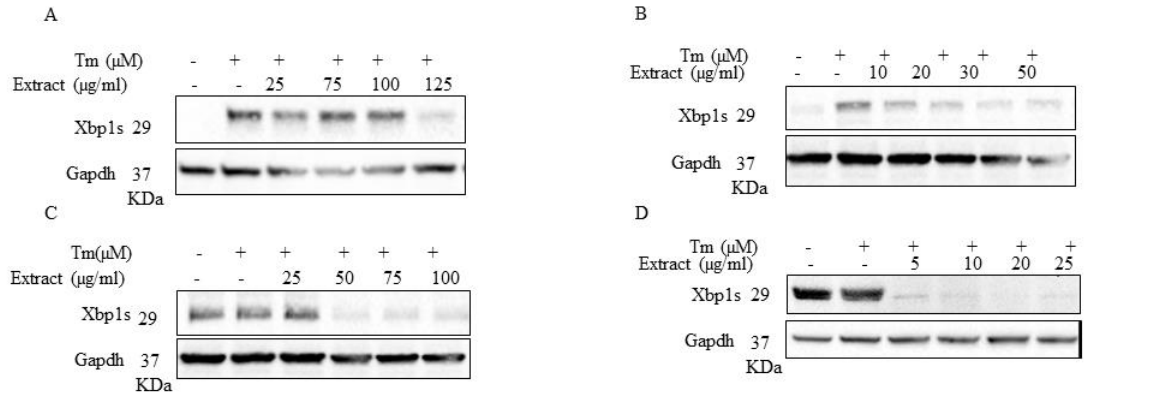

530

531 **Figure.5: Immunoblot analysis for Xbp1-s in (A) Hek293T (B) MDAMB 231(C)**
532 **MCF 7 (D) U87 MG:** Protein extracts of Hek T 293, MDAMB 231, MCF 7 and
533 U87MG stimulated with or without 6µM Tunicamycin (4hr) for induction of Unfolded
534 Protein Response followed by treatment with different concentrations in µg/ml of ANME
535 was isolated and run out for Western blotting. Blots were probed with Xbp1s. GAPDH
536 was used as loading control. Experiments were repeated three times and a representative
537 blot is shown.

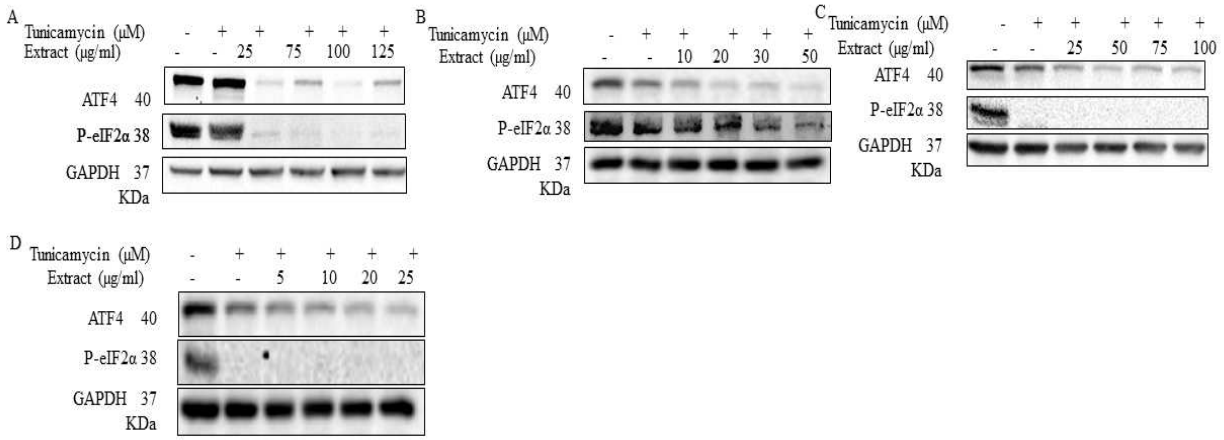

538

539 **Figure.6: Immunoblot analysis for p-eIF2α and ATF4 (A) Hek293T (B) MDAMB**
540 **231(C) MCF 7 (D) U87 MG:** Protein extracts of Hek T 293, MDAMB 231, MCF 7 and

U87MG stimulated with or without 6µM Tunicamycin (4hr) for induction of Unfolded Protein Response followed by treatment with different concentrations in µg/ml of ANME was isolated and run out for Western blotting. Blots were probed with Xbp1s. GAPDH was used as loading control. Experiments were repeated three times and a representative blot is shown.

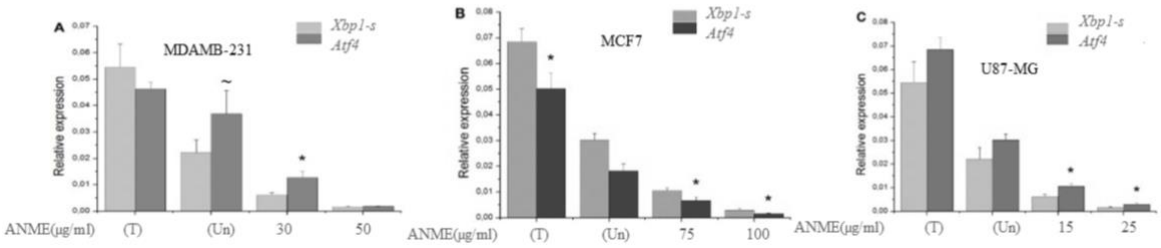

Figure.7: Quantitative real time PCR for relative expression of UPR markers, Xbp1 and ATF4: (A-C) MDAMB-231, MCF 7 and U87-MG . Cells were treated with Tm (6 µg/ml) for 4h followed by treatment with different concentrations in µg/ml of ANME. *Xbp1 and ATF4* mRNA levels were measured by RT-quantitative PCR (qPCR). Measurements were normalized to *ACTB* mRNA ($n = 3$). (* - $p < 0.05$, ~ - $p < 0.1$).

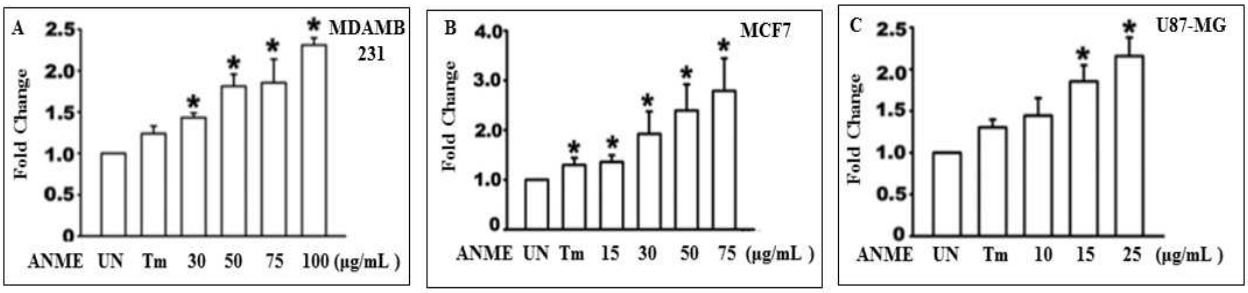

Figure.8: Quantitative real time PCR for relative expression of RIDD marker, Blos1S1 (A-C) MDAMB-231, MCF 7 and U87-MG . Cells were treated with Tm (6 µg/ml) for 4h followed by treatment with different concentrations in µg/ml of ANME.

*Blos1S1*mRNA levels were measured by RT-quantitative PCR (qPCR). Measurements were normalized to *ACTB* mRNA ($n = 3$). (* - $p < 0.05$).

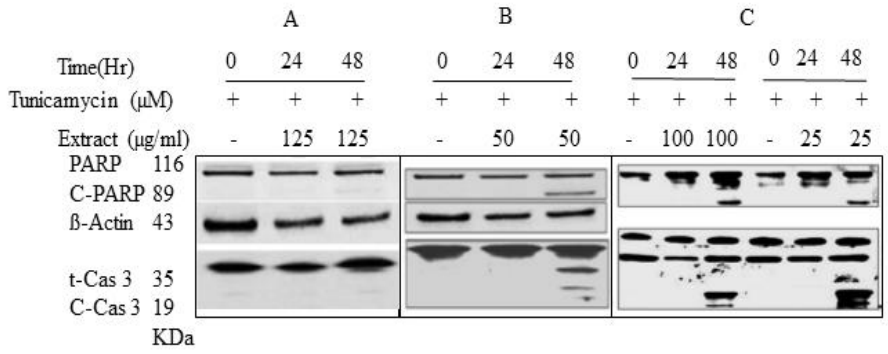

Figure.9: Activation of caspases by ANME: Protein expression of anti- Caspase 3 and anti- PARP using ANME in (A) HEK- 293T (B) U87 MG (C) MDAMB231 and MCF7 cells, resp. Protein extracts of HEK T 293, U87 MG, MDAMB 231 and MCF7 stimulated with or without 6µM Tunicamycin for induction of Unfolded Protein Response followed by treatment with different concentrations of ANME were isolated and run out for Western blotting. Blots were probed with anti- Caspase 3 and anti- PARP. GAPDH was used as loading control. Experiments were repeated three times and a representative blot is shown.

References:

1. Mudasar Ahmad, Zahoor A. Kaloo1, Bashir A. Ganai, Ubaid Yaqoob , Hilal A. Ganaie (2017). **Phytochemical Screening of Aquilegia nivalis Flax Jackson: An Important Medicinal Plant of Kashmir Himalaya: A Perspective**, Adv. Biomed. Pharma. 4:1, 6-12
2. Chandra Prakash Kala (2006) **Medicinal plants of the high altitude cold desert in India: Diversity, distribution and traditional uses,** The International Journal of Biodiversity Science and Management, 2:1, 43-56

3. Adamska T, Młynarczyk M, Jodynis-Liebert J, Bylka W, Matławska I, 2003. **Hepatoprotective effect of the extract and isocytisoside from *Aquilegia vulgaris*.** Phytotherapy research 17(6), 691-696.
4. Jadwiga Jodynis-Liebert, Teresa Adamska, Małgorzata Ewertowska, Wiesława Bylka, Irena Matławska, 2009. **Aquilegia vulgaris extract attenuates carbon tetrachloride-induced liver fibrosis in rats**, Experimental and Toxicologic Pathology, 61(5) 443-451.
5. Sekena H. A., Aziza A. E., Ibrahim A. B., Mohamed I. M. and Mosaad A. W., 2011. **Aquilegia vulgaris extract protects against the oxidative stress and the mutagenic effects of cadmium in Balb/c mice**, Experimental and Toxicologic Pathology, 63(4), 337-344.
6. Purushotham, G., Padma, Y., Nabiha, Y. *et al.* 2016.. **In vitro evaluation of anti-proliferative, anti-inflammatory and pro-apoptotic activities of the methanolic extracts of *Andrographis nallamalayana* Ellis on A375 and B16F10 melanoma cell lines.** *3 Biotech* (6) 212.
7. Younis Mohammad Hazari, Arif Bashir, Ehtisham ul Haq, Khalid Majid Fazili., 2016. **Emerging tale of UPR and cancer: an essentiality for malignancy.** Tumor Biology, 37, 11, 14381-14390
8. Chevet, E., Hetz, C., Samali, A., 2015. **Endoplasmic Reticulum Stress-Activated Cell Reprogramming in Oncogenesis**. Cancer Discov. 5, 586-597
9. Dejeans, N., Barroso, K., Fernandez-Zapico, M.E., Samali, A., Chevet, E., 2015. **Novel roles of the unfolded protein response in the control of tumor development and aggressiveness**. Semin Cancer Biol. 33, 67-73.
10. Hetz, C., Chevet, E., Oakes, S.A., 2015. **Proteostasis control by the unfolded protein response**. Nat Cell Biol. 17, 829-38.

11. Balch, W.E., Morimoto, R.I., Dillin, A., Kelly, J.W., 2008. **Adapting proteostasis for disease intervention**. Science. 319, 916-9.

12. Bartoszewska, S., Collawn, J.F., 2020. **Unfolded protein response (UPR) integrated signaling networks determine cell fate during hypoxia.** Cell Mol Biol Lett 25, 18

13. Schubert, U., Anton, L.C., Gibbs, J., Norbury, C.C., Yewdell, J.W., Bennink, J.R., 2000. **Rapid degradation of a large fraction of newly synthesized proteins by proteasomes.** Nature. 404, 770-4.

14. Claudio Hetz and Feroz R. Papa, 2018., **The Unfolded Protein Response and Cell Fate Control**., Molecular cell, 69, 2, 169-181,

15. Samirul Bashir, Mariam Banday, Ozaira Qadri, Arif Bashir, Nazia Hilal, Nida-i-Fatima, Stephen Rader, Khalid Majid Fazili, 2021., **The molecular mechanism and functional diversity of UPR signaling sensor IRE1**, Life Sciences,, Volume 265,, 2021, 118740

16. Greenman C, Stephens P, Smith R, Dalgliesh GL et al. 2007. **Patterns of somatic mutation in human cancer genomes.** Nature. 8; 446(7132),153-8.

17. Guichard C, Amaddeo G, Imbeaud S, Ladeiro Y, Pelletier L, Maad IB, Calderaro J, Bioulac-Sage P, Letexier M, Degos F, Clément B, Balabaud C, Chevet E, Laurent A, Couchy G, Letouzé E, Calvo F, Zucman-Rossi J. 2012. **Integrated analysis of somatic mutations and focal copy-number changes identifies key genes and pathways in hepatocellular carcinoma.** Nat Genet. 44(6), 694-8.

18. Parsons DW, Jones S, Zhang X, Lin JC et al. 2008. **An integrated genomic analysis of human glioblastoma multiforme.** Science. 321(5897),1807-12.

19. Ortiz-Urda S, Garcia J, Green CL, Chen L, Lin Q, Veitch DP, Sakai LY, Lee H, Marinkovich MP, Khavari PA. 2005. **Type VII collagen is required for Ras-driven human epidermal tumorigenesis.** Science. 307(5716), 1773-6.

20. Snuderl M, Fazlollahi L, Le LP, Nitta M, Zhelyazkova BH, Davidson CJ, Akhavanfard S, Cahill DP, Aldape KD, Betensky RA, Louis DN, Iafrate AJ. 2011.

626 **Mosaic amplification of multiple receptor tyrosine kinase genes in glioblastoma.**
627 Cancer Cell. 20(6), 810-7.
628 21. Hanahan D, Weinberg RA. 2011. **Hallmarks of cancer: the next generation.**
629 Cell. 144(5), 646-74.
630 22. Venditti R, Scanu T, Santoro M, Di Tullio G, Spaar A, Gaibisso R, Beznoussenko
631 GV, Mironov AA, Mironov A Jr, Zelante L, Piemontese MR, Notarangelo
632 A, Malhotra V, Vertel BM, Wilson C, De Matteis MA. 2012. **Sedlin controls the ER**
633 **export of procollagen by regulating the Sar1 cycle.** Science. 337(6102), 1668-72.
634 23. Levental KR, Yu H, Kass L, Lakins JN, Egeblad M, Erler JT, Fong SF, Csiszar
635 K, Giaccia A, Weninger W, Yamauchi M, Gasser DL, Weaver VM. 2009. **Matrix**
636 **crosslinking forces tumor progression by enhancing integrin signaling.**
637 Cell. 139(5),891-906.
638 24. Shi, Z., Yu, X., Yuan, M. et al., 2019., **Activation of the PERK-ATF4 pathway**
639 **promotes chemo-resistance in colon cancer cells**. Sci Rep 9, 3210
640 25. Hart LS, Cunningham JT, Datta T, Dey S, Tameire F, Lehman SL, Qiu B, Zhang H,
641 Cerniglia G, Bi M, Li Y, Gao Y, Liu H, Li C, Maity A, Thomas-Tikhonenko A, Perl
642 AE, Koong A, Fuchs SY, Diehl JA, Mills IG, Ruggero D, Koumenis C. 2012, **ER**
643 **stress-mediated autophagy promotes Myc-dependent transformation and tumor**
644 **growth**. J Clin Invest.,122, 12, 4621-34.
645 26. Rozpedek W, Pytel D, Mucha B, Leszczynska H, Diehl JA, Majsterek I. The Role of
646 the PERK/eIF2α/ATF4/CHOP **Signaling Pathway in Tumor Progression During**
647 **Endoplasmic Reticulum Stress**. Curr Mol Med. 2016;16(6):533-44.
648 27. Huber AL, Lebeau J, Guillaumot P, Pétrilli V, Malek M, Chilloux J, Fauvet F, Payen
649 L, Kfoury A, Renno T, Chevet E, Manié SN.,2013, **p58(IPK)-mediated attenuation**
650 **of the proapoptotic PERK-CHOP pathway allows malignant progression upon**
651 **low glucose**. Mol Cell, 49, 6, 1049-59.

28. Arif Bashir, Younis Hazari, Debnath Pal, Dibyajyoti Maity, Samirul Bashir, Laishram Rajendrakumar Singh, Naveed Nazir Shah, Khalid Majid Fazil, 2020., **Aggregation of M3 (E376D) variant of alpha1- antitrypsin**. Sci Rep 10, 8290

29. Anderson D. J. et al. 2015. **Targeting the AAA ATPase p97 as an approach to treat cancer through disruption of protein homeostasis.** Cancer Cell (28), 653–665.

30. Chou TF. 2011. **Reversible inhibitor of p97, DBeQ, impairs both ubiquitin-dependent and autophagic protein clearance pathways.** Proc. Natl. Acad. Sci. USA (108), 4834–4839.

31. Benosman S. 2013 **Interleukin-1 receptor-associated kinase-2 (IRAK2) is a critical mediator of endoplasmic reticulum (ER) stress signaling.** *PloS one* 8; e64256.

32. Tam AB. Koong AC. & Niwa M. 2014. **Ire1 has distinct catalytic mechanisms for XBP1/HAC1 splicing and RIDD.** Cell reports (9, 850–858.

33. Hamid Bakshi , Smitha Sam, Roya Rozati, Phalisteen Sultan, Tajamul Islam, Babita Rathore, Zahoor Lone, Manik Sharma, Jagrati Triphati, Ramesh Chand Saxena, 2010. **DNA fragmentation and cell cycle arrest: a hallmark of apoptosis induced by crocin from kashmiri saffron in a human pancreatic cancer cell line;** Asian Pac J Cancer Prev. 2010;11(3):675-9.

34. Albrahim T & Alnasser M & Al-Anazi, Mashael & Alkahtani, Muneera & Alkahtani, Saad & Al-Qahtani, Ahmed. 2020. **Potential anti-inflammatory and anti-apoptotic effect of Coccinia grandis plant extract in LPS stimulated-THP-1 cells.** Environmental Science and Pollution Research. 27. 10.1007/s11356-020-08445-5.

35. Ashok Singh , Manohar Lal & S. S. Samant (2009) **Diversity, indigenous uses and conservation prioritization of medicinal plants in Lahaul valley, proposed Cold Desert Biosphere Reserve, India,** International Journal of Biodiversity Science & Management, 5:3, 132-154

36. Ewertowska M, Jodynis-Liebert J, Kujawska M, Adamska T, Matławska I, Szaufer-Hajdrych M., 2009, **Effect of Aquilegia vulgaris (L.) ethyl ether extract on liver antioxidant defense system in rats.** Int J Occup Med Environ Health, 22(2):115-23.
37. Marina Potest, Antonella Minutolo, Angelo Gismondi, Lorena Canuti, Maurice Kenzo, Valentina Roglia, Federico Macchi, Sandro Grelli, Antonella Canini, Vittorio Colizzi, Carla Montesano. 2019. **Cytotoxic and apoptotic effects of different extracts of *Moringa oleifera* Lam on lymphoid and monocytoid cells**, Experimental and Therapeutic Medicine, 5-17
38. Li, S., Pasquin, S., Eid, H. M., Gauchat, J. F., Saleem, A., & Haddad, P. S. 2018. **Anti-apoptotic potential of several antidiabetic medicinal plants of the eastern James Bay Cree pharmacopeia in cultured kidney cells**. *BMC complementary and alternative medicine*, *18*(1), 37.
39. Kowalczyk, T., Sitarek, P., Skała, E., Toma, M., Wielanek, M., Pytel, D., Wieczfińska, J., Szemraj, J., & Śliwiński, T. 2019. **Induction of apoptosis by in vitro and in vivo plant extracts derived from Menyanthes trifoliata L. in human cancer cells.** *Cytotechnology*, *71*(1), 165–180.
40. Fribley, A., Zhang, K., & Kaufman, R. J. (2009). **Regulation of apoptosis by the unfolded protein response.** ***Methods in molecular biology*** *(Clifton, N.J.)*, *559*, 191–204. https://doi.org/10.1007/978-1-60327-017-5_14
41. Raffaella Iurlaro and Cristina Munoz-Pinedo.2016. **Cell death induced by endoplasmic reticulum stress**, FEBS Journal 283, 2640–2652
42. Bartoszewska, S., Collawn, J.F. 2020. **Unfolded protein response (UPR) integrated signaling networks determine cell fate during hypoxia**. *Cell Mol Biol Lett* (25), 18
43. Wang L, Perera BG, Hari SB, Bhhatarai B, Backes BJ, Seeliger MA. 2012. **Divergent allosteric control of the IRE1alpha endoribonuclease using kinase inhibitors.** Nat Chem Biol. (8), 982–9.

44. Bouchecareilh M, Higa A, Fribourg S, Moenner M, Chevet E. 2011. **Peptides derived from the bifunctional kinase/RNase enzyme IRE1alpha modulate IRE1alpha activity and protect cells from endoplasmic reticulum stress.** FASEB J. (25),3115–29.

45. Arvin B. Tam, Lindsay S. Roberts, Vivek Chandra, Io Guane Rivera, Daniel K. Nomura, Douglass J. Forbes, Maho Niwa 2018, **The UPR Activator ATF6 Responds to Proteotoxic and Lipotoxic Stress by Distinct Mechanisms** . Developmental Cell 46, 327–343

46. Anna Shemorry ,Jonathan M Harnoss, Ofer Guttman, Scot A Marsters, László G Kőműves, David A Lawrence, Avi Ashkenazi (2019) **Caspase-mediated cleavage of IRE1 controls apoptotic cell commitment during endoplasmic reticulum stress** eLife 2019;8:e47084

47. Anna Walczak, Kinga Gradzik, Jacek Kabzinski, Karolina Przybylowska-Sygut, Ireneusz Majsterek, 2019, **The Role of the ER-Induced UPR Pathway and the Efficacy of Its Inhibitors and Inducers in the Inhibition of Tumor Progression,** Oxidative Medicine and Cellular Longevity, 2019, 5729710, 1-15

48. Emma Madden , Susan E. Logue , Sandra J. Healy , Serge Manie , Afshin Samali, 2019. **The role of the unfolded protein response in cancer progression: From oncogenesis to chemoresistance**, Biology of the Cell, 111,1,1-17.

49. Upton JP, Wang L, Han D, Wang ES, Huskey NE, Lim L, Truitt M, McManus MT, Ruggero D, Goga A, Papa FR, Oakes SA. 2012. **IRE1α cleaves select microRNAs during ER stress to derepress translation of proapoptotic Caspase-2.** Science. 338, 6108, 818-22.

50. Bi M, Naczki C, Koritzinsky M, Fels D, Blais J, Hu N, Harding H, Novoa I, Varia M, Raleigh J, Scheuner D, Kaufman RJ, Bell J, Ron D, Wouters BG, Koumenis C.,2005. **ER**

stress-regulated translation increases tolerance to extreme hypoxia and promotes tumor growth. EMBO J. 24, 19

Figures

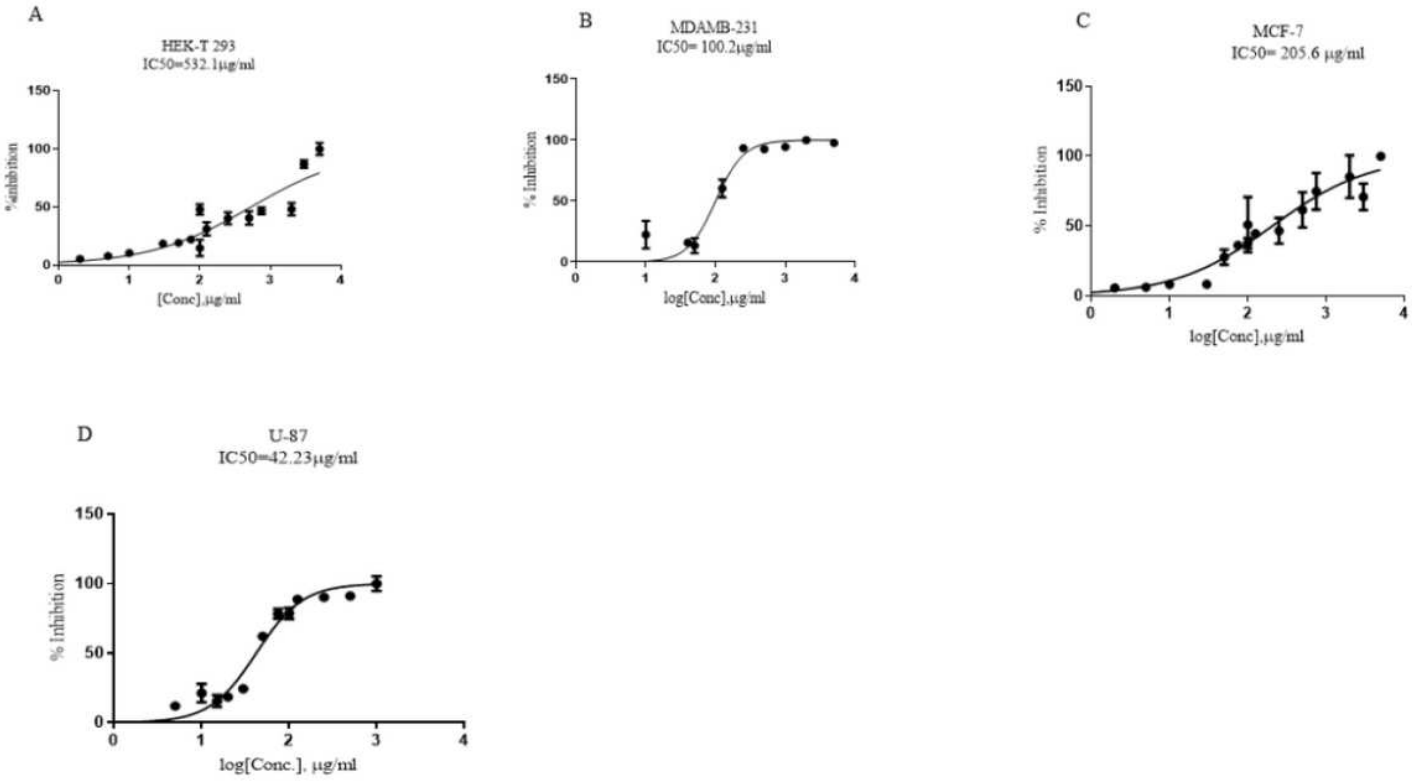

Figure 1

Effect of ANME on (A)HekT293 (B) MDAMB-231(C) MCF7 and (D) U87MG 2 cells in various concentrations (1-2000µg/mL) after 24 hours; determined using MTT cell viability assay: Dose–response curves of ANME was determined using MTT cell viability assay. IC50 values were calculated as mean values from three independent experiments by nonlinear regression using Graph pad Prism®6 software. Percentage inhibition of untreated cells was assumed to be zero.

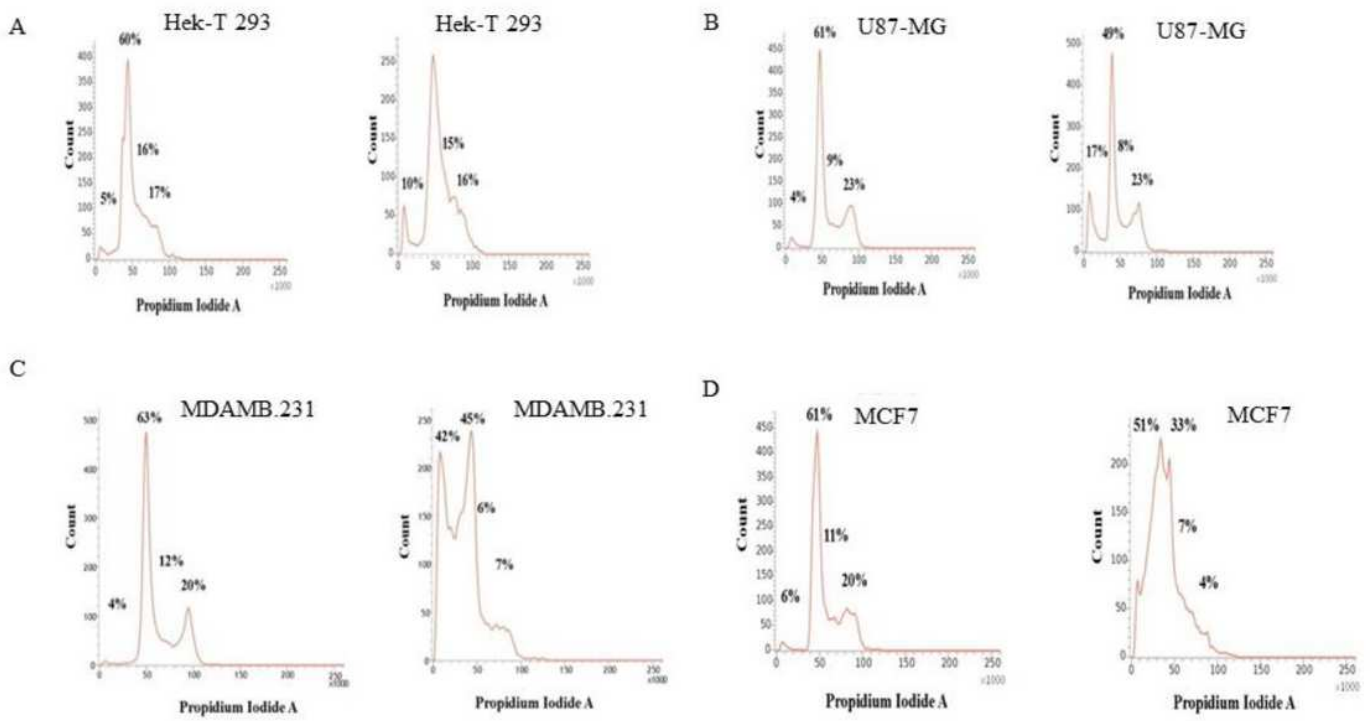

Figure 2

Cell cycle analysis: (A-D) Hek293T, U87, MDAMB-231 and MCF 7 cell lines were treated with different concentrations of ANME for 24 hrs and cells were fixed and stained with propidium iodide and analyzed by flow cytometry. The mean values ± SD were calculated from three different experiments. $p<0.05$ with respect to control.

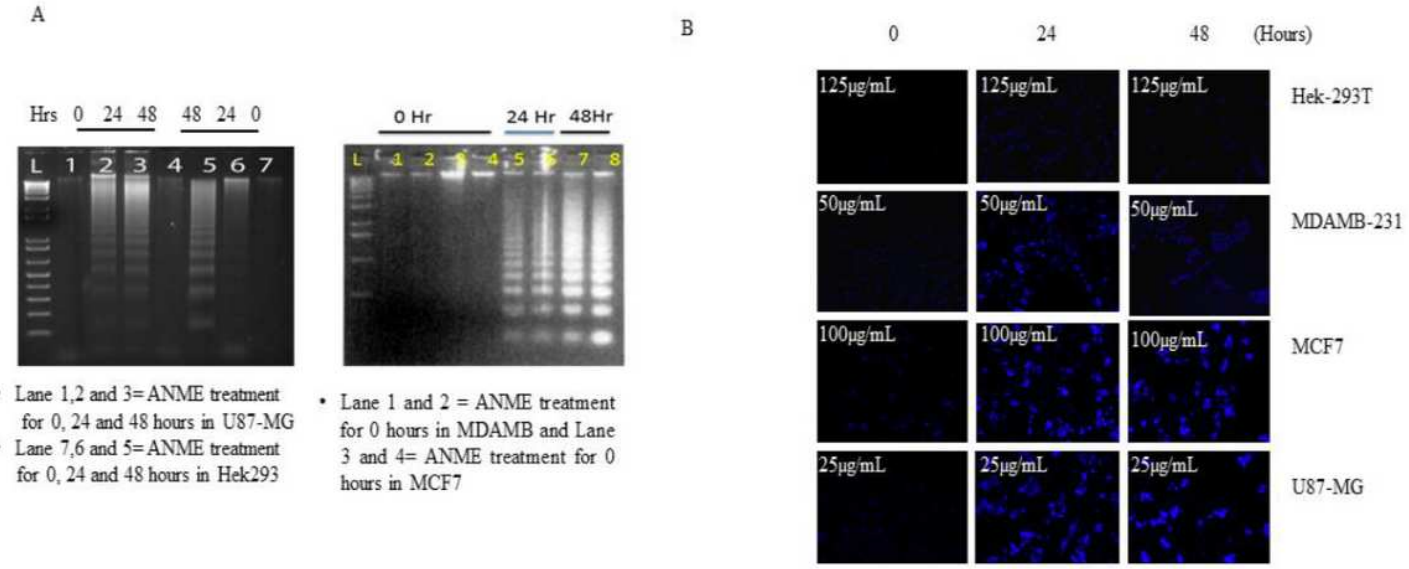

Figure 3

(A) Time dependent DNA fragmentation: DNA Laddering in (a) U87- MG and HEK-T293 cells (b) MDAMB231 and MCF7 cells resp. ANME extract induces DNA fragmentation in all the cell line panels stimulated with or without 6μM Tunicamycin(4hr) for induction of Unfolded Protein cells. The cells were treated with different concentrations (μg/ml) of extract for every cell type for 0, 24 and 48 h. Cells from each sample were harvested for DNA gel electrophoresis as described; (B)Formation of apoptotic bodies in time dependent manner, DAPI staining:Morphological and nuclear changes induced by ANME. HEK-T293, MDAMB, MCF7 and U87-MG cells after treatment with different concentration for each cell type induced various nuclear changes such as chromatin condensation, nuclei condensation, and nuclear degradation, as demonstrated by DAPI staining at 400× in time dependent manner. However Hek293 showed only inhibition in cell growth with no signs of apoptosis; ANME=Aquilegia nivalis methanolic extract.

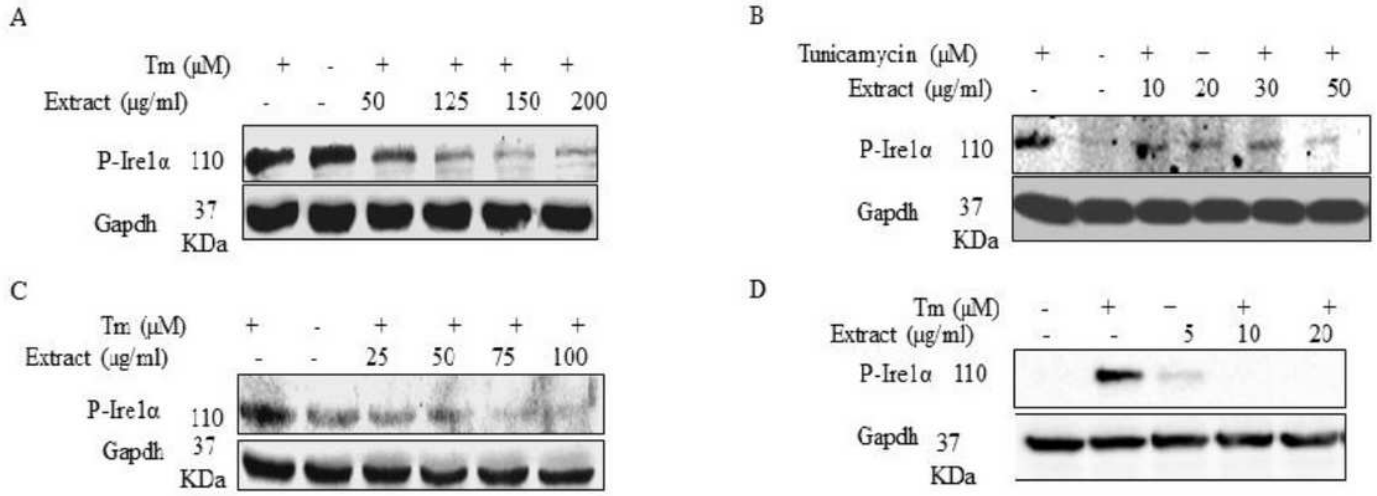

Figure 4

Immunoblot analysis for p-Ire1α in (A) Hek293T (B) MDAMB 231(C) MCF 7 (D) U87 MG: Protein extracts of Hek T 293, MDAMB 231, MCF 7 and U87MG stimulated with or without 6μM Tunicamycin (4hr) for induction of Unfolded Protein Response followed by treatment with different concentrations in μg/ml of ANME was isolated and run out for Western blotting. Blots were probed with p-Ire1 α. GAPDH was used as loading control. Experiments were repeated three times and a representative blot is shown.

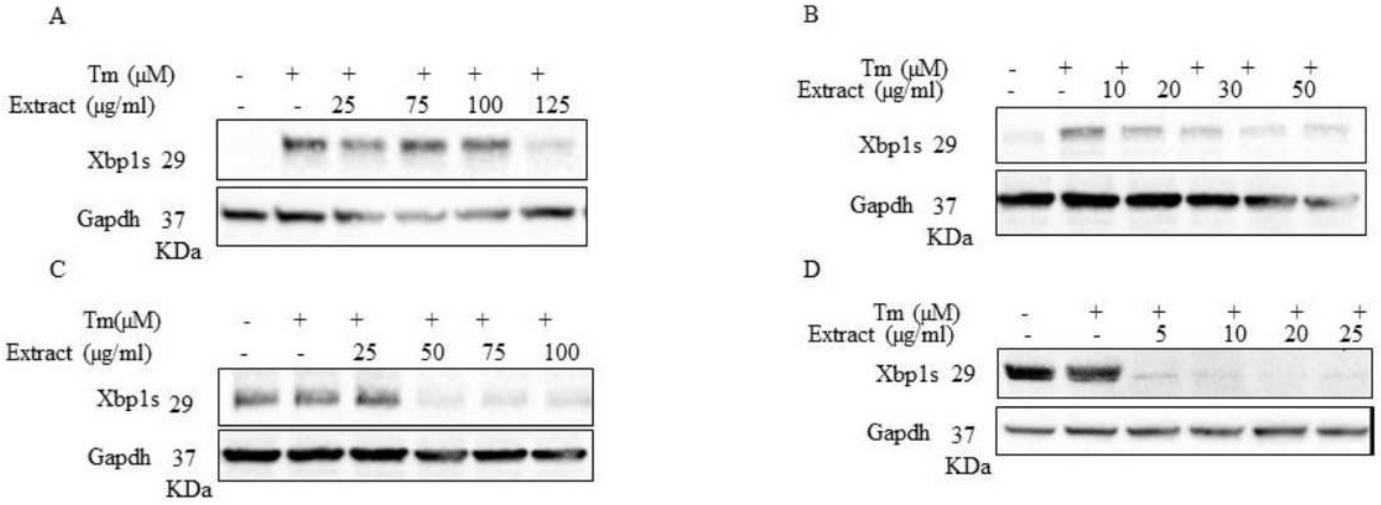

Figure 5

Immunoblot analysis for Xbp1-s in (A) Hek293T (B) MDAMB 231(C) MCF 7 (D) U87 MG: Protein extracts of Hek T 293, MDAMB 231, MCF 7 and U87MG stimulated with or without 6µM Tunicamycin (4hr) for induction of Unfolded Protein Response followed by treatment with different concentrations in µg/ml of ANME was isolated and run out for Western blotting. Blots were probed with Xbp1s. GAPDH was used as loading control. Experiments were repeated three times and a representative blot is shown.

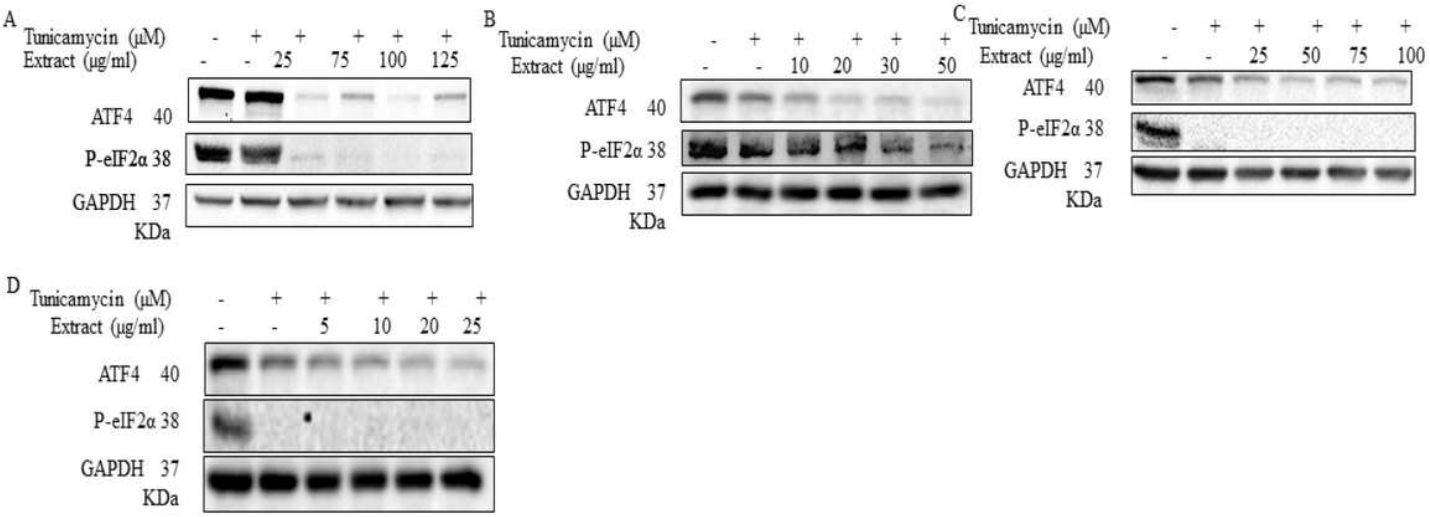

Figure 6

Immunoblot analysis for p-eIF2α and ATF4 (A) Hek293T (B) MDAMB 231(C) MCF 7 (D) U87 MG: Protein extracts of Hek T 293, MDAMB 231, MCF 7 and U87MG stimulated with or without 6µM Tunicamycin (4hr) for induction of Unfolded Protein Response followed by treatment with different concentrations in

µg/ml of ANME was isolated and run out for Western blotting. Blots were probed with Xbp1s. GAPDH was used as loading control. Experiments were repeated three times and a representative blot is shown.

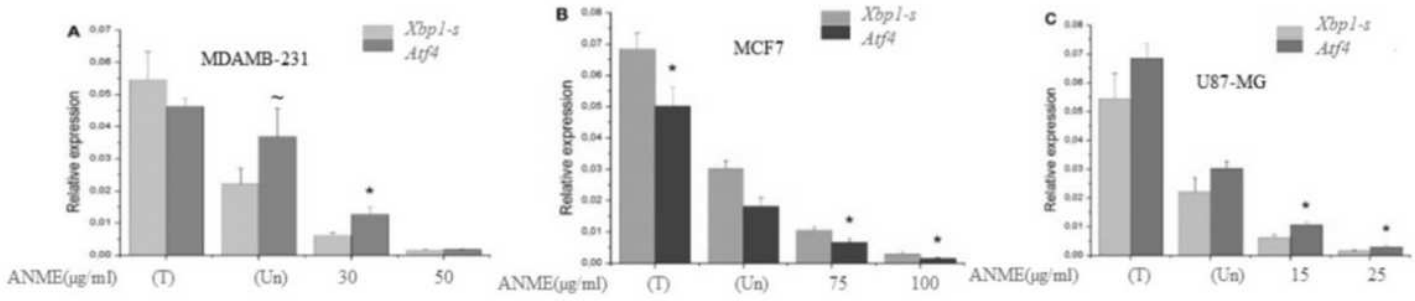

Figure 7

Quantitative real time PCR for relative expression of UPR markers, Xbp1 and ATF4: (A-C) MDAMB-231, MCF 7 and U87-MG . Cells were treated with Tm (6 µg/ml) for 4h followed by treatment with different concentrations in µg/ml of ANME. Xbp1 and ATF4 mRNA levels were measured by RT-quantitative PCR (qPCR). Measurements were normalized to ACTB mRNA (n = 3). (* - p < 0.05, ~ - p < 0.1).

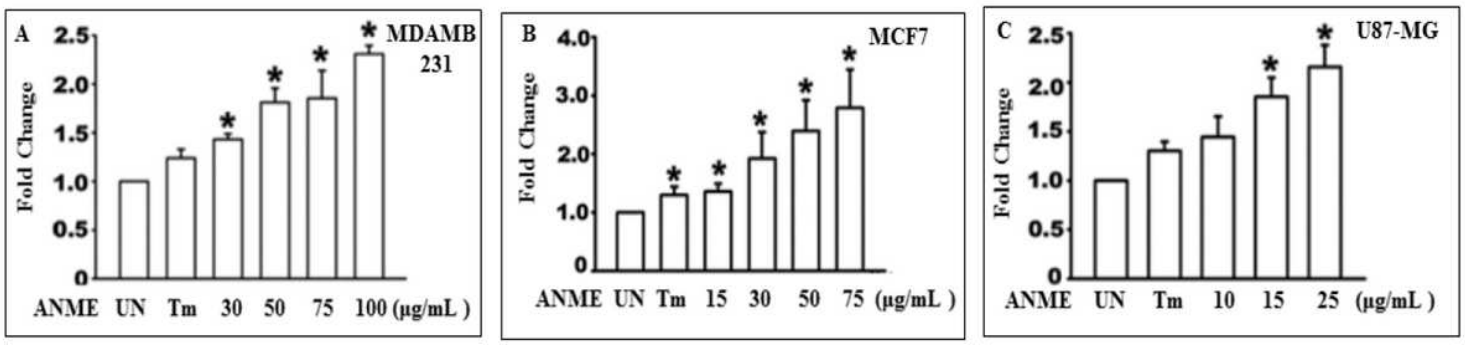

Figure 8

Quantitative real time PCR for relative expression of RIDD marker, Blos1S1 (A-C) MDAMB-231, MCF 7 and U87-MG . Cells were treated with Tm (6 µg/ml) for 4h followed by treatment with different concentrations in µg/ml of ANME. Blos1S1mRNA levels were measured by RT-quantitative PCR (qPCR). Measurements were normalized to ACTB mRNA (n = 3). (* - p< 0.05).

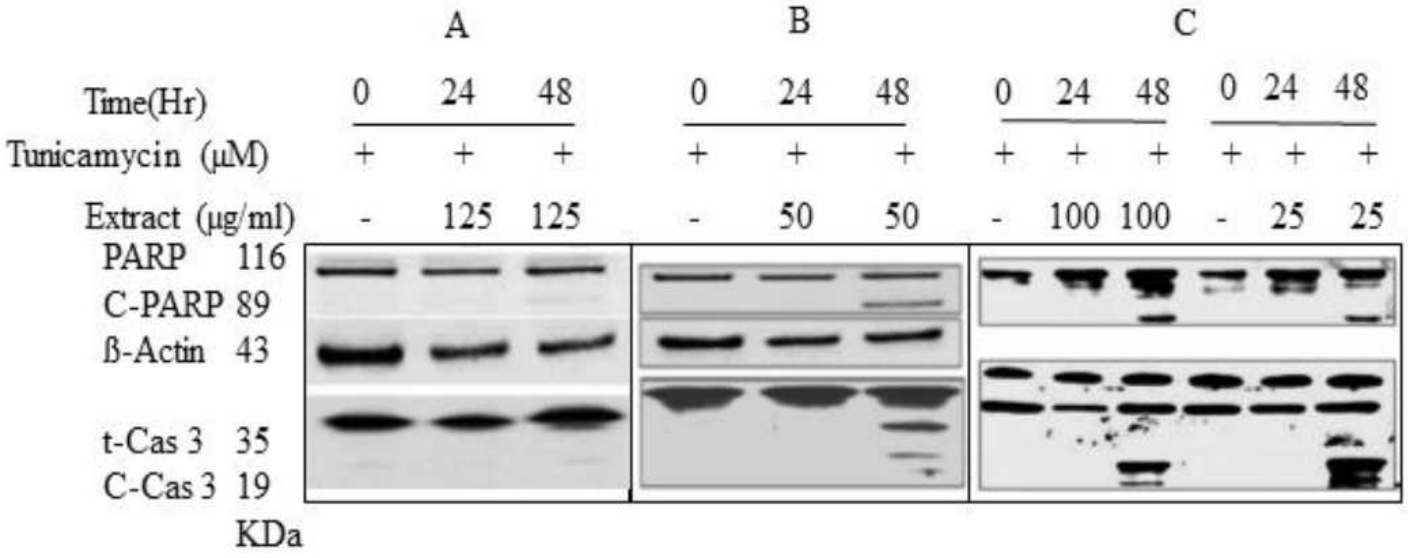

Figure 9

Activation of caspases by ANME: Protein expression of anti- Caspase 3 and anti- PARP using ANME in (A) HEK- 293T (B) U87 MG (C) MDAMB231 and MCF7 cells, resp. Protein extracts of HEK T 293, U87 MG, MDAMB 231 and MCF7 stimulated with or without 6µM Tunicamycin for induction of Unfolded Protein Response followed by treatment with different concentrations of ANME were isolated and run out for Western blotting. Blots were probed with anti- Caspase 3 and anti- PARP. GAPDH was used as loading control. Experiments were repeated three times and a representative blot is shown.